Chapter 7 Hollow Fe_2O_3–TiO_2–PtO_x Nanostructure with Two Distinct Cocatalysts Embedded Separately on Two Surface Sides for Efficient Visible Light Water Splitting to Hydrogen

Minh-Hao Pham,[†] Cao-Thang Dinh,[†] Gia-Thanh Vuong,[†] Ngoc-Don Ta,[‡] and Trong-On Do*,[†]

[†]*Department of Chemical Engineering, Laval University, Quebec City, Quebec G1V 0A6, Canada*

[‡] *School of Chemical Engineering, Hanoi University of Science and Technology, Hanoi, Vietnam*

Submitted to a refereed journal

Résumé

Un nouveau nanocomposite oxyde métallique–TiO_2–PtO_x de forme creuse a été synthétisé en utilisant des nanocristaux de MIL-88B comme un tensioactif solide dans lequel, la structure est composée de centres $Fe_3(\mu_3–O)$ liés par coordination insaturée. Les sites acides de Lewis sur la surface des nanocristaux du MIL-88B, qui sont formés par la déshydratation des centres trimériques métalliques $Fe_3(\mu_3–O)$, sont greffés en premier par le précurseur du titane contenant le groupe amine via l'attachement de leur atome d'azote par des paires d'électrons avec les sites acides de Lewis. Ceci conduit à la déposition d'une couche mince de TiO_2 sur la MIL-88B surface. Après calcination, le nanocomposite composé d'un hybride Fe_2O_3–TiO_2 creux avec l'épaisseur de mur contrôlable (15 – 30 nm) est préparé. De plus, deux fonctions catalytiques distinctes (oxydation et réduction) qui sont séparément localisées localisés sur deux opposites surfaces du creux: une comme Fe_2O_3 issue à partir de la structure MOF par calcination embarquée à l'intérieur de la surface du creux, et l'autre par le dopage du métal tel que PtO_x sur le côté extérieur de la surface du creux. Ce nanocomposite creux non seulement absorbe la lumière visible, mais aussi améliore la séparation des électrons et trous photogénérés, due à l'épaisseur de paroi mince et les deux co-catalyseurs (Fe_2O_3 and PtO_x) localisés sur deux opposites surfaces du creux. En conséquence, ce type de nano-composites est très performant pour la production d'H_2 à partir de l'eau sous la lumière visible.

Abstract

A new hollow hybrid metal-oxide–TiO_2–PtO_x nanocomposite was synthesized by using MIL-88B nanocrystals consisting of coordinatively unsaturated metal centers $Fe_3(\mu_3–O)$ as template. Lewis acid sites on the surface of the MIL-88B nanocrystals, which were formed from the dehydrated trimeric metal centers, were first grafted with titanium precursor containing amine group via attaching their nitrogen atoms with lone pairs of electrons. This led to the successful deposition of TiO_2 thin shell on the MIL-88B. The calcined hollow nanocomposite is composed of hybrid metal oxide–TiO_2 with controllable wall thickness (15 – 30 nm) and two distinct functional (oxidative and reductive) cocatalysts that are separately located on two different surface sides of the hollow: one as Fe_2O_3 from the iron-based MOF nanocrystal via calcination embedded inside of hollow surface, and the other by metal-doping such as PtO_x on the outside of hollow surface. This hollow nanocomposite not only absorbs visible light, but also enhances the separation between photogenerated electrons and holes due to the thin wall thickness and the surface separation of two distinct functional cocatalysts. As a result, an efficient visible-light photo-activity of this nanocomposite is found for the H_2 production from water.

7.1 Introduction

Because of the depletion of fossil fuels and the serious environmental problems accompanying their combustion, a new form of energy that is clean, renewable, low-cost and a viable alternative to fossil fuels is urgently needed.[1] The solar-driven splitting of water to produce H_2 with semiconductor photocatalysts represents an attractive pathway toward solving important energy and environmental problems.[2] However, the significant challenge of using sunlight for H_2 generation lies in designing an efficient system using visible rather than UV light.

To achieve high efficiency, a sunlight driven photocatalyst is usually composed of semiconductor that harvests visible light and cocatalysts that are loaded and highly dispersed on the photocatalyst surface to create active sites and reduce the activation energy for gas formation. The cocatalysts are typically a noble metal such as Pt and Rh as reductive sites for H_2 evolution and metal oxide such as iron oxide and manganese oxide as oxidative sites.[2,3] Upon band gap excitation in the photocatalyst, the photogenerated electrons and holes migrate toward the reductive and oxidative surface sites, respectively, thereby facilitating efficient electrons-holes separation. This photocatalytic system thus improves the photocatalytic activity for water splitting, as compared to those of the photocatalyst loading either reduction or oxidation cocatalyst.[4] Furthermore, the two distinct cocatalysts, which are highly dispersed and isolated from each other onto the same photocatalyst, are highly desired to promote water splitting in harmony under visible light irradiation. However, to date, the demonstration of this concept still remains a major challenge.[5]

Among the semiconductor-based photocatalysts (e.g., titanium dioxide,[6] oxide solid solutions,[7] and tantalum-nitrogen compounds[8] etc.), TiO_2 is considered to be the most possible candidate for commercial scale-up due to inexpensive, nontoxic and robust photocatalyst under photochemical conditions. Due to its large band gap (3.0 eV and 3.2 eV for rutile and anatase, respectively), TiO_2 only absorbs UV light. Several approaches, including doping with transition metals such as Fe, Cr, Cu or non-metals, N, S, C or

hydrogenation have been taken to narrow the band gap of TiO_2 and thus extends the photoactivity in visible region.[9] Alternatively, the coupling of TiO_2 with narrow band gap semiconductors could also result in visible light-induced photoactivities.[10]

On the other hand, metal organic–frameworks (MOFs), which are formed by polymeric connections of metal centers as "clusters" in coordination with organic linkers, have emerged as an interesting class for diverse applications such as gas storage, gas separation, catalysis, chemical sensing and drug delivery,[11] owing to their incredibly tunable physical and chemical properties as well as rationally tailored crystal morphologies.[12] Among them, various MOF structures consist of coordinatively unsaturated metal centers (namely, MOF-UMCs) such as trimeric $Cr_3(\mu_3–O)$ or $Fe_3(\mu_3–O)$ clusters of MIL-88 and MIL-101. Each trimeric metal(III) center in the MOF frameworks possesses terminal water molecules that can be removed by vacuum and temperature treatements to provide Lewis acid sites. These dehydrated UMCs are very beneficial to grafting organic molecules or trapping gases, because of their strong interactions with electron-rich functional groups. Among them, amine functional groups are often used as grafting units.[13]

Herein, we report a novel approach to develop a new type of hollow metal oxide–TiO_2 nanostructure using nanocrystals of MOF-UMCs as hard template. This type of nanocomposite is composed of hollow hybrid metal oxide–TiO_2 with controllable hollow wall thickness (15-30 nm) and two distinct functional (*i.e.* oxidative and reductive) cocatalysts that are separately located on two hollow surface sides: one of which, *i.e.* metal oxide from MOF template via calcination, embedded inside of hollow surface and the other by metal doping such as PtO_x outside of hollow surface. This hollow nanocomposite not only absorbs visible light, but also greatly enhances photogenerated electron/hole separation because of the hollow thin wall and the isolation of the two distinct functional cocatalysts. As a result, a highly efficient visible-light photo-activity is found for the H_2 production from water.

To illustrate our approach, we have selected iron-based MIL-88B nanocrystal consisting of unsaturated $Fe_3(\mu_3–O)$ clusters as a hard template, titanium (IV) (triethanolaminato)

isopropoxide $C_3H_7OTi(OC_2H_4)_3N$ with amine group (namely, TEAI) as a grafting reagent and H_2PtCl_6 as a Pt source for the synthesis of a hollow α-Fe_2O_3–TiO_2–PtO_x nanostructure. Lewis acid sites are created from the UMCs of the MIL-88B framework after removal of terminal water molecules by vacuum/temperature treatment, to which TEAI with amine group can be grafted via the lone electron pair of nitrogen atom (Scheme 7.1). Even though numerous Lewis acid sites are available in the dehydrated framework, because of the dense state of MIL-88B,[14] TEAI is grafted on its outer surface. To increase the shell titania thickness, TEAI-grafted MIL-88B nanocrystals were treated with a dilute solution of TEAI in ethanol with 5 vol % H_2O. During this treatment, the hydrolysis and condensation of TEAI produce MIL-88B core/TiO_2 shell nanostructure. The thickness of the titania shell can be also controlled by the TEAI concentration.

Scheme 7.1 Schematic illustration of the procedure for the design of hollow α-Fe_2O_3–TiO_2–PtO_x photocatalysts with two cocatalysts separate from each other using MIL-88B nanocrystals containing UCMs as the hard template for visible light-induced water splitting into hydrogen.

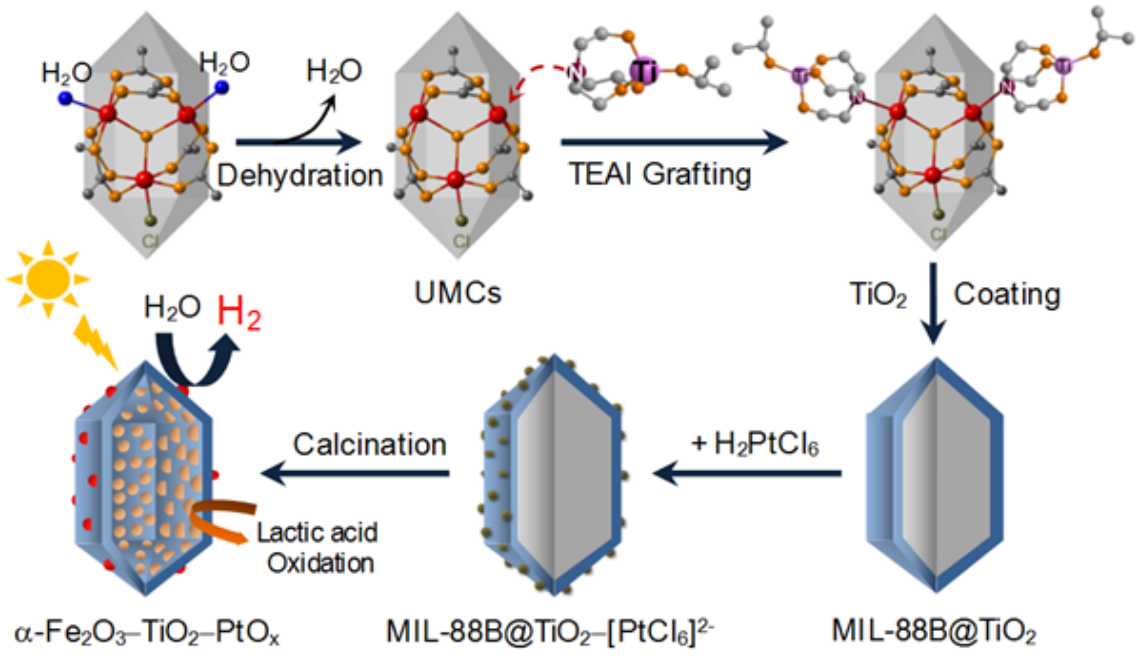

7.2 Results and discussion

In a typical procedure, MIL-88B nanocrystals with desired size were prepared by following the method described in our previous work, by using $FeCl_3 \cdot 6H_2O$, 2-amino-1,4-benzene dicarboxylic acid, Pluronic F127 and acetic acid.[15] The resulted bipyramidal hexagonal prism crystals with an average length of ~500 nm and width of ~150 nm are shown in Figure 7.1a, b and Figure S7.1a. The MIL-88B structure with the formula of $Fe_3O(H_2N–BDC)_3Cl(H_2O)_2$ was also confirmed by the powder X-ray diffraction (Figure S7.1b).

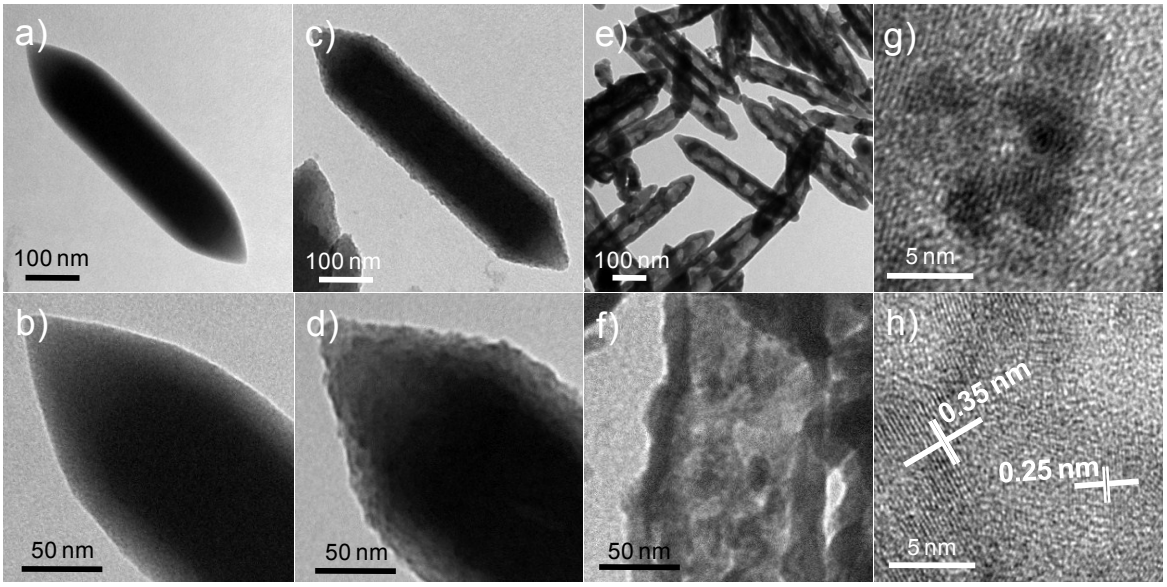

Figure 7.1 TEM and HRTEM images of MIL-88B (a, b); MIL-88B@TiO_2 (c, d) and hollow α-Fe_2O_3-TiO_2-PtO_x (e-h).

In the MIL-88B framework, each $Fe_3(\mu_3–O)$ cluster contains two terminal water molecules, after removal of these water molecules by a dehydration treatment, Lewis acid sites are created and available for amine grafting.[16] TEAI-grafted MIL-88B nanocrystals were achieved by treating the dehydrated MIL-88B with solution of TEAI in 2-propanol. TEM images indicate no essential change in morphology of the TEAI-grafted nanocrystals as compared to that of the pristine MIL-88B sample (Figure S7.2a, b). However, the presence

of Ti was found as indicated by X-ray photoelectron spectroscopy (XPS) because of the TEAI molecules anchoring on the MIL-88B outer surface (Figure S7.2c). Subsequently, the TEAI-grafted MIL-88B nanocrystals were treated in refluxing dilute solution of TEAI in ethanol (5 vol % H_2O). Because of the grafting, hydrolysis and condensation of TEAI, MIL-88B core/TiO_2 shell nanostructure with controllable titania shell thickness can be obtained. As seen by TEM images, the as-made obtained MIL-88B core/titania shell nanomaterial exhibits the same morphology of the pristine MIL-88B (Figure 7.1c, d and Figure S7.3a). However, this material shows a rough surface instead of the smooth surfaces of the pristine sample, which indicates the formation of titania shell on MIL-88B. The XPS spectrum also indicates a large amount of Ti on this sample (Figure S7.3b). The powder XRD pattern of the as-made MIL-88B core/titania shell nanoparticles shows only diffraction peaks which are characteristic of the MIL-88B structure (Figure 7.2a); no diffraction peak that is characteristic of TiO_2 was observed, indicating the amorphous TiO_2 shell. This is also confirmed by the HRTEM observation (Figure S7.3a – inset).

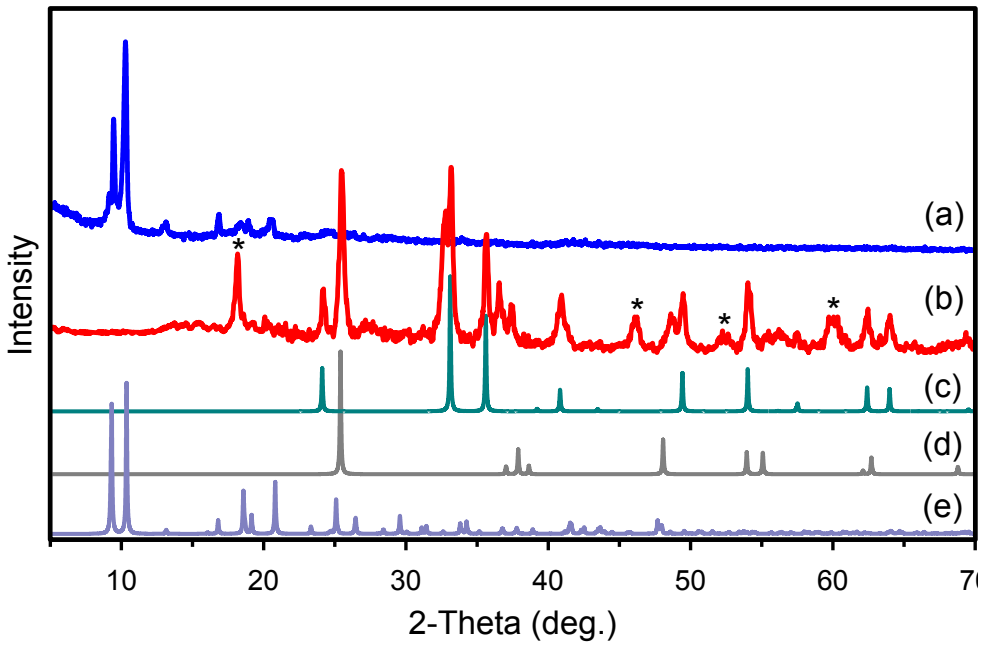

Figure 7.2 Powder XRD patterns of MIL-88B@TiO_2 (a), α-Fe_2O_3–TiO_2–PtO_x (b) and simulated patterns for α-Fe_2O_3 (c), anatase TiO_2 (d), MIL-88B (e) for references.

In order to generate the hollow photocatalyst with two cocatalysts located on two distinct sides, the as-made MIL-88B core/titania shell nanomaterial was loaded with H_2PtCl_6 by wet impregnation, followed by calcination in air. After the calcination, the color of this sample changed from dark brown to dark red, because of the decomposition of Fe-based MIL-88B core into iron oxide. Importantly, no essential change in morphology of this sample after the calcination was observed, as showed by TEM (Figure 7.1e) and SEM (Figure S7.4) images; however, shrinkage in size was found. The TEM image exhibits clearly a hollow nanostructure with a mean wall thickness of 15 nm. Note that under the same calcination conditions, the pristine MIL-88B nanocrystals (i.e., without titania shell) were destroyed, forming aggregated irregular iron oxide particles (Figure S7.5). The TEM and HRTEM images show PtO_x nanoparticles with the size of 3 – 4 nm dispersed on the hollow surface (Figure 7.1f, g). Because of solid MIL-88B@TiO_2 core-shells, H_2PtCl_6 only embedded on their outer surface, and thus PtO_x cocatalyst located on the outer side of the hollow. HRTEM image also indicates that each individual hollow nanoparticle is composed of metal oxides that are well crystallized with d-spacing of 0.35 nm matching the d_{101} of anatase TiO_2, and of 0.25 nm matching the d_{110} of α-Fe_2O_3 (Figure 7.1h).

XRD pattern of the hollow α-Fe_2O_3–TiO_2–PtO_x sample shows diffraction peaks that match those of anatase TiO_2 and α-Fe_2O_3 phases (Figure 7.2b). Four additional peaks (asterisked in Figure 7.2b) of this sample are the characteristic of Fe-titanate mixed oxide (Fe_2TiO_5), which could be formed at the interface of TiO_2 and α-Fe_2O_3.

The formation of the hollow structure and the shrinkage of the MIL-88B core/titania shell structure after the calcination are attributed to the decomposition of the MIL-88B core into iron oxide nanoparticles that occupy much less volume, and the transformation of amorphous phase to crystalline phase of TiO_2 shell under the thermal treatment in air, as demonstrated by the thermogravimetric analysis (Figure S7.6). N_2 sorption isotherm of the hollow α-Fe_2O_3–TiO_2–PtO_x sample indicates the BET surface area of 40 m^2/g.

The thickness of Fe_2O_3–TiO_2 hybrid wall can be controlled by adjusting the concentration of TEAI in the refluxing solution. When the TEAI concentration increases from 6 mM to

50 mM the thickness increases from 15 nm to 30 nm (Figure 7.1f and Figure S7.8). However, at high concentrations of TEAI, isolated TiO_2 nanoparticles were formed.

XPS was also recorded to investigate the chemical states of Ti and Fe in the hollow α-Fe_2O_3–TiO_2–PtO_x material (Figure 7.3). The Ti2p spectrum fitted with Gaussian-Lorentzian function reveals obviously a dominant $Ti2p_{3/2}$ peak with binding energy (BE) at 458.0 eV, which is characteristic of Ti^{4+} state in TiO_2 lattice,[17] along with two shoulders. The first shoulder at 456.5 eV corresponds to Ti^{3+} state because of oxygen deficiency in TiO_2[18] whilst the second shoulder at 458.6 eV arises from Ti^{4+} state in Ti–O–Fe structure.[19] In the Ti–O–Fe bond, the Pauling electro-negativity differential between Fe^{3+} (1.83) and Ti^{4+} (1.54) ions induces the possibility of electron transfer from Ti^{4+} to Fe^{3+}, which makes Ti^{4+} ion less electron and Fe^{3+} more electron rich and thus results in an increase of core electron BE of Ti^{4+} and a decrease of core electron BE of Fe^{3+}. For the XPS spectrum of Fe2p, three dominant peaks: Fe $2p_{3/2}$ at 712.1 eV, Fe $2p_{1/2}$ at 725.5 eV and a satellite peak at 719.1 eV are in accord with the presence of α-Fe_2O_3.[20] Moreover, the fitted Fe $2p_{3/2}$ peak showed an additional peak at 710.3 eV, which is assigned to Fe^{3+} state in the Ti–O–Fe bond. The absence of Fe $2p_{3/2}$ peak at 709.3 eV suggests that no Fe^{2+} is present in the sample.

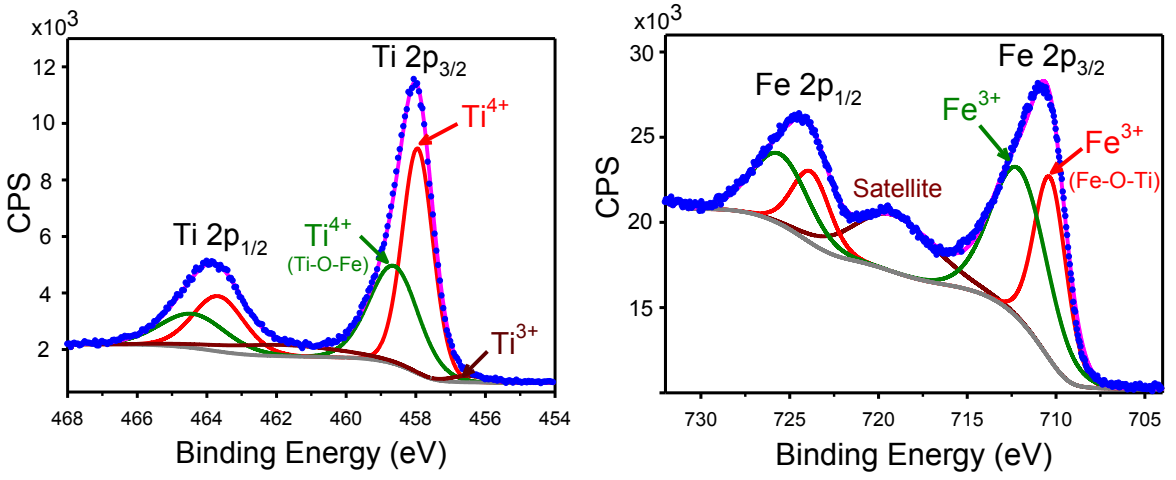

Figure 7.3 XPS spectra of Ti 2p and Fe 2p core levels of the hollow α-Fe_2O_3–TiO_2–PtO_x.

The presence of Ti^{4+} and Fe^{3+} states in the Ti–O–Fe bond suggests Fe-doping in the TiO_2 lattice. It is inferred that during the calcination, the MIL-88B core is decomposed. In parallel, the amorphous shell is conversed to crystalline titania one and iron ions from the MIL-88B enter into the TiO_2 lattice, producing Fe-doped TiO_2. Because of high iron content in MIL-88B@TiO_2, iron oxide nanoparticles are also formed inside of the Fe-doped TiO_2 shell. The XPS analysis, which probes only a few nanometres deep of the surface, indicates the surface Ti/Fe atomic ratio of 1:1.9, whereas the bulk Ti/Fe atomic ratio calculated from EDS is 1:4.0, corresponding to 20 wt % TiO_2 and 80 wt % Fe_2O_3. These results indicate that the hollow particle is rich in Fe and some α-Fe_2O_3 segments inside, however, is rich in Ti outside of hollow Fe_2O_3–TiO_2.

UV-vis diffuse reflectance spectrum of the hollow α-Fe_2O_3–TiO_2–PtO_x nanostructure exhibits the absorbance in visible region with a band edge around 610 nm (Figure 7.4, left). The absorption onset is similar to that of α-Fe_2O_3 with a band gap at 2.0 eV.[21] Therefore, the visible light absorption of the hollow hybrid could be attributed to α-Fe_2O_3, Fe-doped TiO_2 and Fe_2TiO_5, in which the visible light absorption of Fe-doped TiO_2 overlaps with that of α-Fe_2O_3 and Fe_2TiO_5.

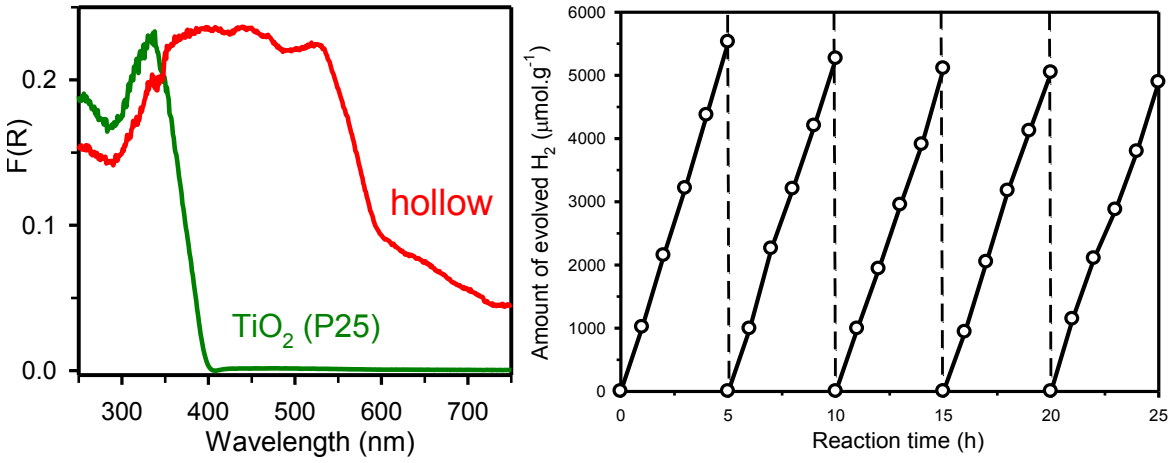

Figure 7.4 UV-vis diffuse reflectance spectrum (left) and the photoactivity for water splitting under visible light irradiation (right) of hollow α-Fe_2O_3–TiO_2–PtO_x photocatalyst.

The photocatalytic activity of the hollow α-Fe_2O_3–TiO_2–PtO_x nanocomposite for hydrogen generation was carried out under visible light irradiation (λ > 420 nm) using lactic acid as sacrificial reagent. The results showed that 1.1 $mmol \cdot h^{-1} \cdot g^{-1}$ of H_2 gas was evolved in this catalytic system. To investigate the stability of α-Fe_2O_3–TiO_2–PtO_x photocatalyst, an experiment of 5 cycles with intermittent N_2 bubbling after every 5 h was carried out without catalyst regeneration. The obtained result indicated an excellent stability for the photocatalyst during the course of the 25 h irradiation without noticeable catalytic deactivity (Figure 7.4, right). The amount of H_2 gas was evolved linearly during the entire period of each cycle, with a total of 5.5 $mmol \cdot g^{-1}$ H_2 produced after 5 h.

For comparison, the composite of α-Fe_2O_3, TiO_2 and PtO_x with the same chemical composition of the hollow α-Fe_2O_3–TiO_2–PtO_x sample was also prepared using the same procedure of synthesis and starting MIL-88B nanocrystals, except that titanium (IV) butoxide (i.e., without amine group) as grafting reagent instead of TEAI. For this calcined sample, under the same photocatalytic conditions, only small quantity of H_2 was produced after the 5 h irradiation. It is obvious that the absence of amine group in the titanium precursor and the rapid hydrolysis of titanium butoxide in ethanol (5 vol % H_2O) led to a physical mixture of TiO_2 particles and MIL-88B nanocrystals rather than MIL-88B@TiO_2 core-shell nanostructure (Figure S7.9). Consequently, no essential hydrogen was formed under visible light for this material. Furthermore, when PtO_x-loaded α-Fe_2O_3 powder prepared from MIL-88B, PtO_x-loaded TiO_2 and PtO_x-loaded Fe_2TiO_5 were used under the same photocatalytic conditions, only trace of H_2 was found in these cases.

Although α-Fe_2O_3 derived from the calcined MIL-88B absorbs visible light, it cannot drive the proton reduction of water because its conduction band is more positive than the potential of $2H^+/H_2$ couple.[22] Similarly, the Fe_2TiO_5 mixed oxide with the CB below the potential of $2H^+/H_2$ cannot reduce the proton. TiO_2 only absorbs UV light and thus does not catalyze the visible light-induced H_2 evolution. The above results demonstrate that Fe-doped TiO_2 thin wall is responsible for the visible light-induced activity of α-Fe_2O_3–TiO_2–PtO_x and the high isolation of α-Fe_2O_3 and PtO_x cocatalysts embedding on

two different sides of the hollow hybrid enhances their photocatalytic activity for water splitting through the efficient separation of photogenerated electrons-holes.

7.3 Conclusions

We have developed an approach toward a new hollow hybrid metal-oxide–TiO_2–PtO_x photocatalyst for visible light-induced water splitting into H_2 by using nanosized MOFs consisting of coordinatively unsaturated metal centers as template. This hollow photocatalyst contains two distinct functional cocatalysts on two different sides of the thin wall. Because of the surface separation of the cocatalysts, the separation between photogenerated electrons and holes is enhanced, resulting in the efficient photocatalysis. This approach can be extended to achieve distinct photocatalysts by varying the chemical composition and morphology of the MOF templates.

7.4 Experimental

Chemicals: $FeCl_3 \cdot 6H_2O$ (Aldrich, 97 %), 2-amino-1,4-benzenedicarboxylic acid (Aldrich, 99 %), Pluronic F127 ($EO_{97}PO_{69}EO_{97}$, average M_n = 12600, Aldrich), CH_3COOH (Fisher, 99.7 %), titanium(IV) (triethanolaminato)isopropoxide (80 wt% in 2-propanol, Aldrich), titanium (IV) butoxide (Aldrich, 97 %), 2-propanol (Aldrich, 99.5 %), ethanol (95 %), $H_2PtCl_6 \cdot 6H_2O$ (Aldrich, ≥ 37.5 % Pt basis) and lactic acid (Aldrich, 85 – 90 % in water). All chemicals were used as received without further purification.

Synthesis of MIL-88B nanocrystals: MIL-88B nanocrystals were prepared by following our previously reported approach.[15] Briefly, the aqueous dispersion (15 mL) of 2-aminoterephtalic acid (60 mg, 0.33 mmol), $FeCl_3 \cdot 6H_2O$ (180 mg, 0.66 mmol), Pluronic F127 (160 mg) and acetic acid (0.6 mL, 10.5 mmol) was heated at 110 ^oC for 24 h. The resulted solid was isolated and washed several times with ethanol by centrifugation to remove the surfactant and excess reactants.

Titanium precursor grafting on MIL-88B nanocrystals: The as-made MIL-88B (100 mg) was dried overnight at 150 ^{o}C under vacuum to remove terminal water molecules. To this dehydrated form, 2 M TEAI solution in 2-propanol (4 mL) was poured and stirred at room temperature for 2 h. The TEAI-grafted MIL-88B was then collected, washed with 2-propanol by centrifugation and dried overnight at 100 ^{o}C.

TiO_2 coating on MIL-88B nanocrystals: TEAI-grafted MIL-88B (100 mg) was dispersed in 80 mL of 6 mM TEAI solution in ethanol (5 vol. % H_2O) and then refluxed for 24 h under vigrous stirring. The MIL-88B@TiO_2 core-shell was collected and washed several times with ethanol by centrifugation.

Preparation of α-Fe_2O_3–TiO_2–PtO_x: 0.57 mL of H_2PtCl_6 aqueous solution (10 mM) was added to the suspension of MIL-88B@TiO_2 (100 mg) in deionized water (12 mL) and stirred for 1 h at room temperature, followed by a rotary evaporation with a water bath at 50 ^{o}C to remove the water. The powder was calcined in air with heating rate at 5 ^{o}C min^{-1} at 500 ^{o}C for 3 h to yield a dark red PtO_x-loaded composite.

Photocatalytic H_2 evolution: Visible light-induced H_2 evolutions were carried out in 300 mL septum-sealed glass reactors. In each run, 20 mg of α-Fe_2O_3–TiO_2–PtO_x was well dispersed with magnetic stirring in a 50 mL of aqueous solution containing lactic acid (10 wt.%). The reactor was deoxygenated by bubbling nitrogen to remove oxygen and then placed in front of a 300 W Xe-lamp with a 420 nm cut-off filter (FSQ-GG420, Newport) under constant stirring. 0.5 mL of the gas in the headspace of the reactor was analyzed by GC to determine the amount of evolved H_2.

Characterizations: Transmission electron microscopy (TEM) images were obtained on a JEOL JEM 1230 microscope operating at 120 kV. High resolution TEM images were performed on a Tecnai G^2 20 instrument operated at 200 kV. Scanning electron microscopy (SEM) images were taken on a JEOL 6360 instrument at an accelerating voltage of 3 kV. Powder X-ray diffraction (XRD) patterns were collected on a Bruker SMART APEX II X-ray diffractometer with Cu Kα radiation (λ = 1.5406 Å) at a scan rate of 1.0^{o} min^{-1}. All

samples were dried at 100 ^{o}C overnight to remove guest solvent molecules within the pores before the XRD scan. XPS measurements were carried out in an ion-pumped chamber (evacuated to 10^{-9} Torr) of a photoelectron spectrometer (Kratos Axis-Ultra) equipped with a focused X-ray source (Al Kα, hν = 1486.6 eV). The UV-vis spectra were recorded on a Cary 300 Bio UV-visible spectrophotometer. N_2 adsorption-desorption isotherms were measured at the temperature of liquid nitrogen with a Quantachrome Autosorb-1 system. The BET surface areas were calculated in the range of 0.05−0.3 P/P_o. Thermogravimetric analysis (TGA) was carried out with a TGA/SDTA 851e thermogravimetric analyzer from room temperature to 600 ^{o}C with a heating rate of 5 ^{o}C min^{-1} under an air flow of 50 mL min^{-1}.

Operation conditions for GC analysis:

Carrier gas: nitrogen at 15 Psi
Column: Carboxen-1010 Plot Capillary 30 m x 0.53 mm.
Detecter: TCD
Column temperature: 30 ^{o}C
Retention time of H_2: 0.9 min

7.5 Appendix

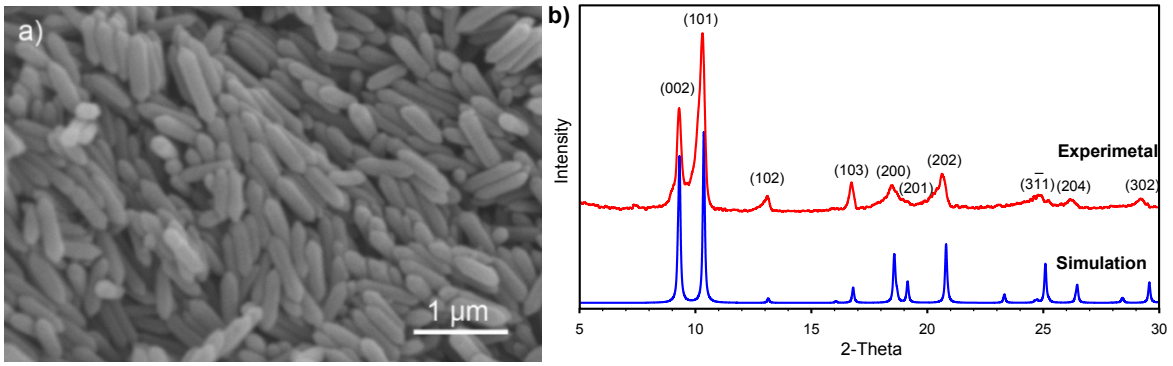

Figure S7.1 SEM image (a) and powder XRD pattern (b) of MIL-88B nanocrystals

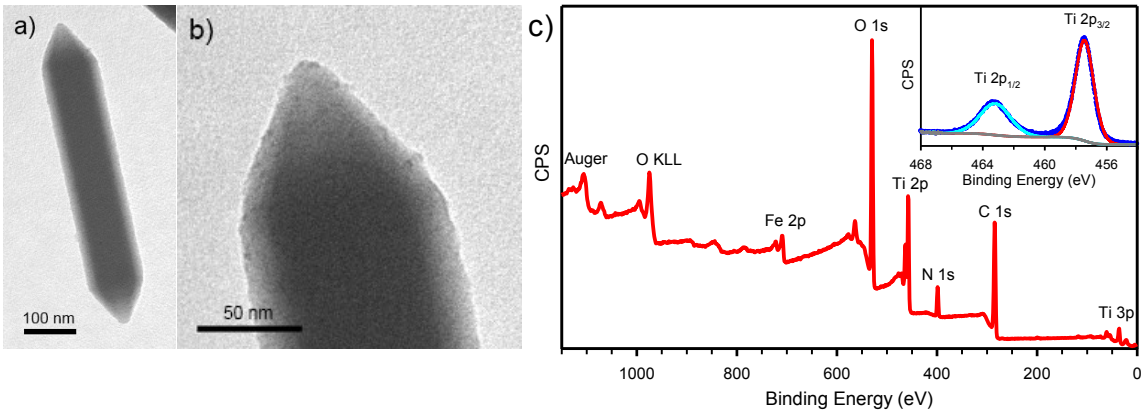

Figure S7.2 TEM images (a, b), XPS survey and high-resolution Ti 2p (inset) spectra (c) of TEAI-grafted MIL-88B nanocrystals.

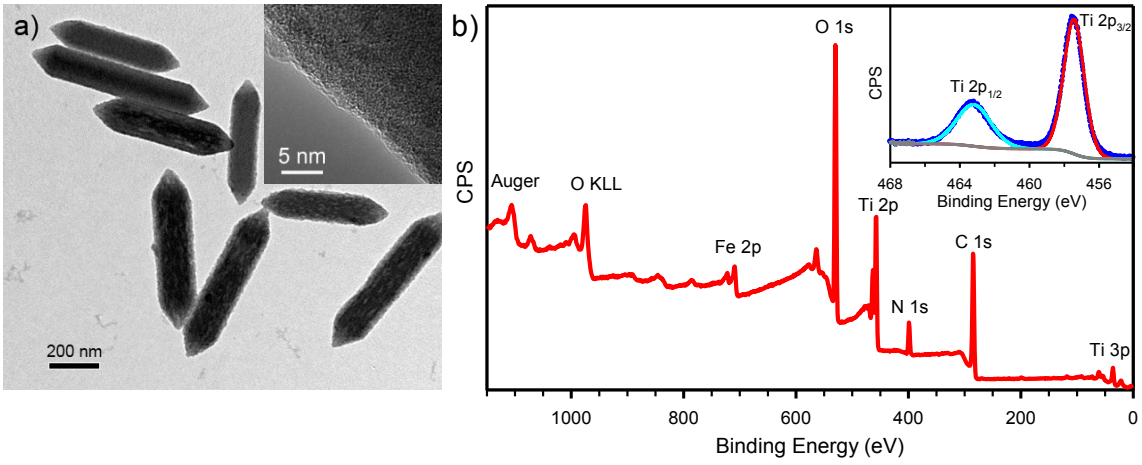

Figure S7.3 TEM and HRTEM (inset) images (a), XPS survey and high-resolution Ti 2p (inset) spectra (b) of MIL-88B@TiO_2 nanoparticles prepared with the concentration of TEAI at 6 mM TEAI.

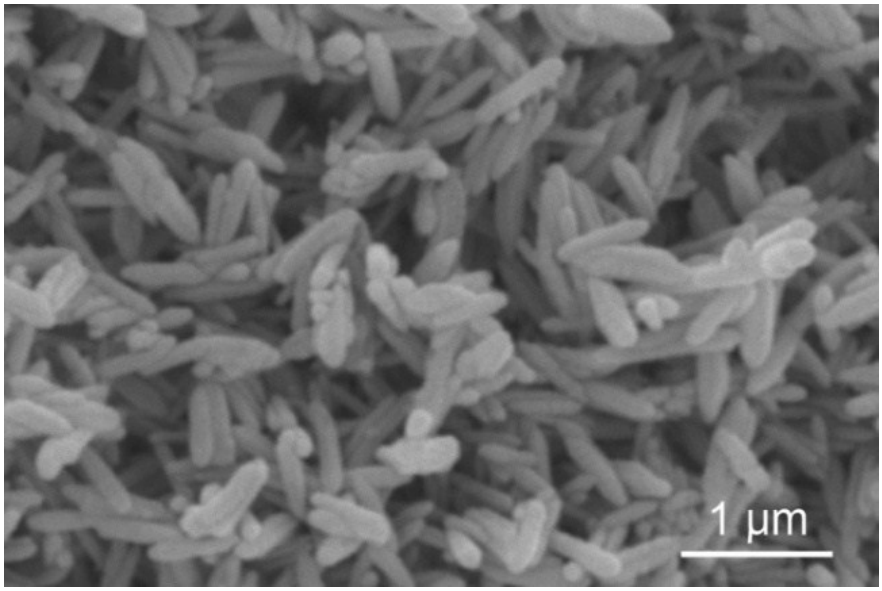

Figure S7.4 SEM image of α-Fe_2O_3–TiO_2–PtO_x sample.

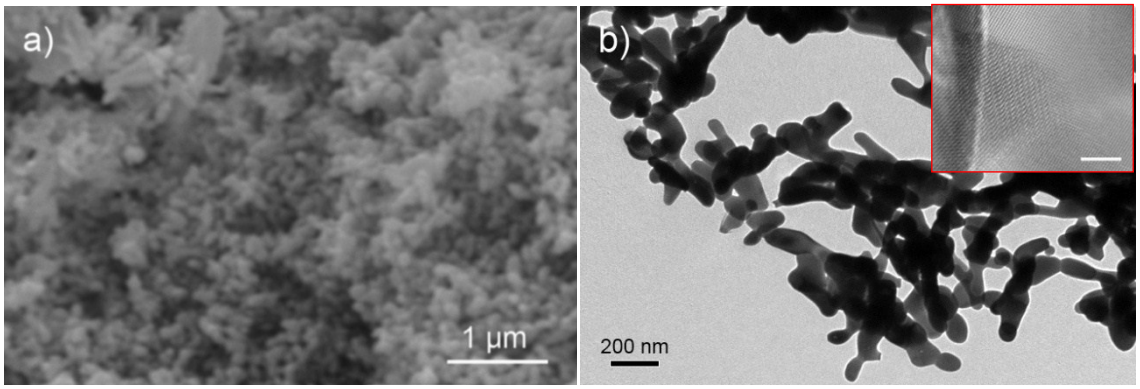

Figure S7.5 SEM (a) and TEM (b) images of iron oxide sample obtained by the calcination of the pristine MIL-88B nanocrystals. HRTEM image (inset) indicates the fusion of iron oxide nanoparticles. The scale bar for the inset is 5 nm.

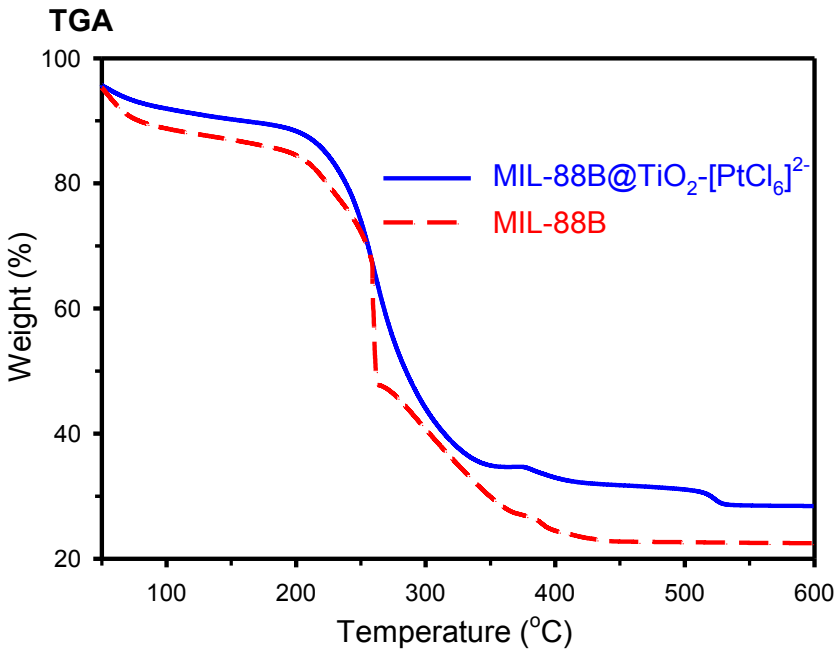

Figure S7.6 The thermogravimetric analysis of MIL-88B and MIL-88B@TiO_2–$[PtCl_6]^{2-}$. The weight retention differential at 500 °C of 8.0 % is attributed to the coated TiO_2 and loaded PtO_x.

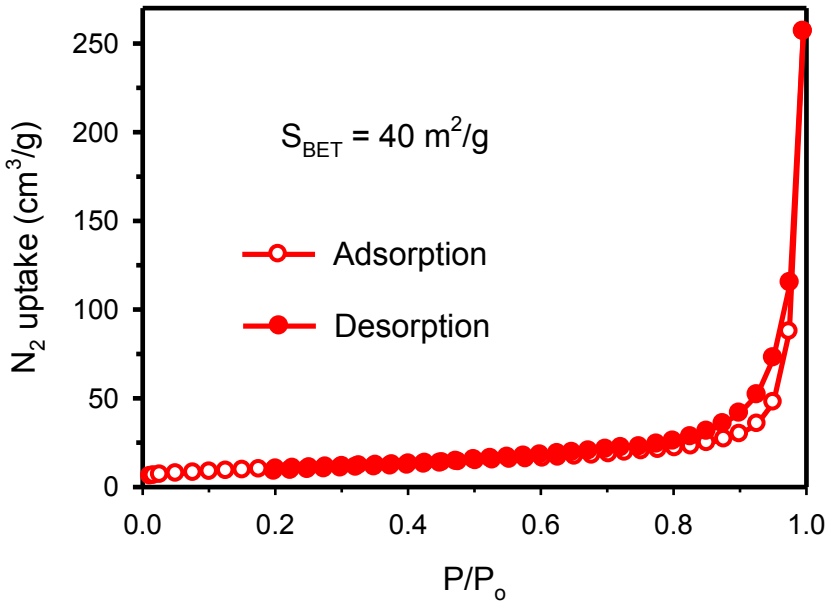

Figure S7.7 N_2 sorption isotherms at 77 K of α-Fe_2O_3–TiO_2–PtO_x.

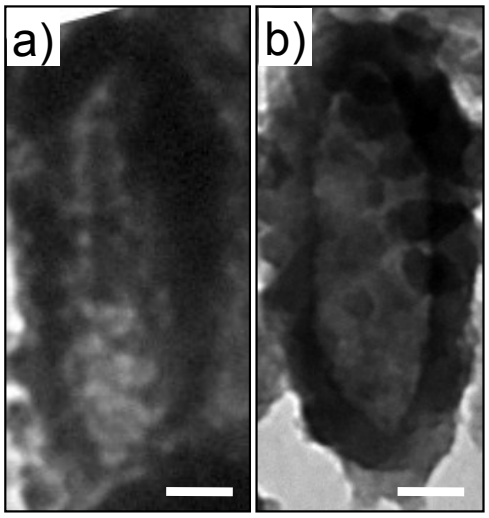

Figure S7.8 The hollow nanoparticles with various thicknesses of Fe_2O_3–TiO_2 hybrid wall prepared with the concentration of TEAI at 25 mM (a) and 50 mM (b) while maintaining other reaction parameters. The scale bar is 50 nm.

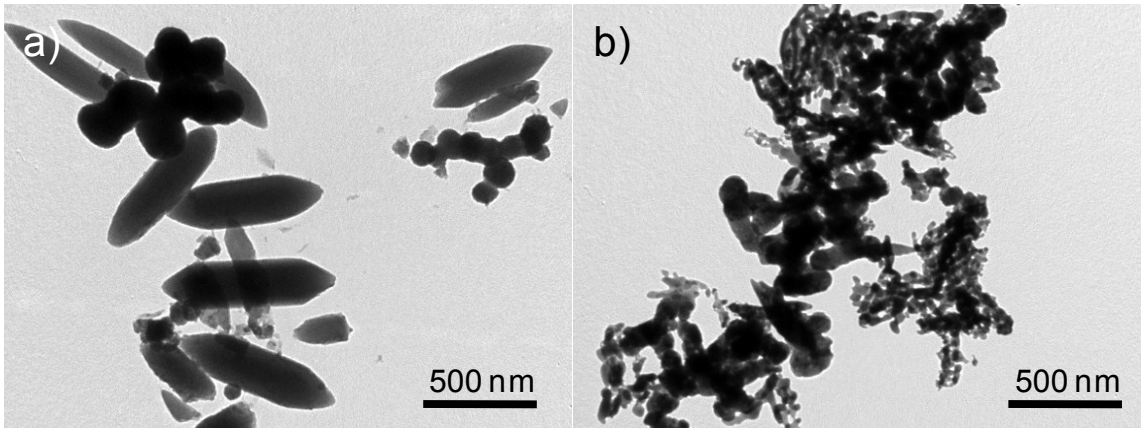

Figure S7.9 TEM images of the sample prepared by using titanium (IV) butoxide without amine group as grafting reagent instead of TEAI before (a) and after the calcination (b). The simple mixtures of TiO_2 nanoparticles and MIL-88B nanocrystals (a) or iron oxide particles (b) were observed instead of MIL-88B core/TiO_2 shell or hollow hybrid nanostructure.